Acta Crystallographica Section F
Structural Biology and Crystallization Communications
ISSN 1744-3091

Molecular cloning, overexpression, purification, crystallization and preliminary X-ray diffraction analysis of a purine nucleoside phosphorylase from *Bacillus subtilis* strain 168

Nadia Helena Martins,‡ Andreia Navarro Meza,‡ Camila Ramos Santos, Priscila Oliveira de Giuseppe and Mario Tyago Murakami*

National Laboratory for Biosciences, Brazilian Synchrotron Light Laboratory, National Center for Research in Energy and Materials, Campinas, Brazil

‡ These authors contributed equally to this work.

Correspondence e-mail: mario.murakami@lnbio.org.br

Received 11 February 2011
Accepted 19 March 2011

Purine nucleoside phosphorylase (PNP; EC 2.4.2.1) is a key enzyme of the purine-salvage pathway. Its ability to transfer glycosyl residues to acceptor bases is of great biotechnological interest owing to its potential application in the synthesis of nucleoside analogues used in the treatment of antiviral infections and in anticancer chemotherapy. Although hexameric PNPs are prevalent in prokaryotes, some microorganisms, such as *Bacillus subtilis*, present both hexameric and trimeric PNPs. The hexameric PNP from *B. subtilis* strain 168, named BsPNP233, was cloned, expressed and crystallized. Crystals belonging to different space groups ($P32_1$, $P2_12_12_1$, $P6_322$ and $H32$) were grown in distinct conditions with pH values ranging from 4.2 to 10.5. The crystals diffracted to maximum resolutions ranging from 2.65 to 1.70 Å.

1. Introduction

Purine nucleoside phosphorylase (PNP; EC 2.4.2.1) is a key enzyme of the purine-salvage pathway that catalyzes the reversible phosphorolysis of purine nucleosides and their analogues, producing the corresponding purine base and ribose 1-phosphate (Fig. 1). Its ability to transfer glycosyl residues to acceptor bases is of great biotechnological interest owing to its potential application in the synthesis of nucleoside analogues used in the treatment of antiviral infections and in anticancer chemotherapy (Li *et al.*, 2008; Nannemann *et al.*, 2010; Visser *et al.*, 2010).

In recent years, eight nucleoside analogues have been approved in the USA for the treatment of AIDS (Clercq, 2009). Moreover, several purine nucleoside analogues have been clinically investigated as potential drugs for the treatment of leukaemia and lymphoma (Ravandi & Gandhi, 2006). However, the production of these molecules still has a high manufacturing cost and faces some challenges such as the low solubility and poor reaction kinetics of the reagents (Visser *et al.*, 2010; Pinheiro *et al.*, 2008). Thus, there is an urgent need to find ways to increase the cost-effectiveness of the synthesis of purine nucleoside analogues.

Use of glycosyl-transferring enzymes such as PNPs can be a good approach to nucleoside synthesis (Koeller & Wong, 2001; Bzowska *et al.*, 2010). Enzyme-catalyzed chemical transformations have been recognized as practical alternatives to nonbiological organic synthesis and as convenient solutions to certain intractable synthetic problems (Koeller & Wong, 2001).

PNPs have been classified into two distinct classes based on their oligomeric state (Pugmire & Ealick, 2002). Members of the NP-I (nucleoside phosphorylase I) family are either trimers or hexamers, whereas members of the NP-II family are dimers. Enzymes belonging to the NP-I family can be further classified according to their substrate specificity and amino-acid sequence. Trimeric PNPs are found in vertebrates and are specific for guanine and hypoxanthine (2′-deoxy)-ribonucleosides. Hexameric PNPs are prevalent in

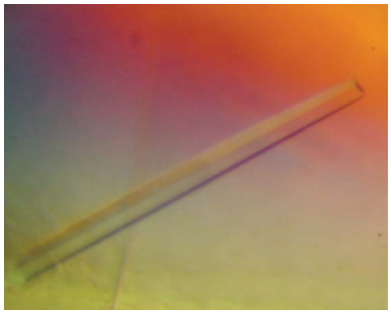

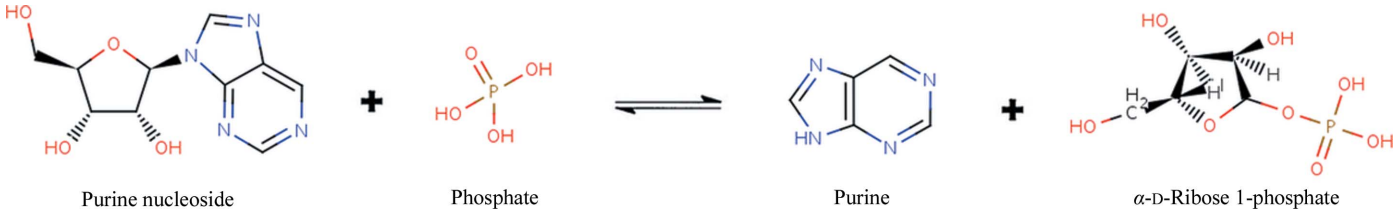

Figure 1
Reaction catalyzed by purine nucleoside phosphorylase (EC 2.4.2.1; Scheer *et al.*, 2011).

prokaryotes and exhibit a broader range of substrates. In some microorganisms, such as *Escherichia coli* and *Bacillus* spp., both a trimeric and a hexameric form of PNP are found (Seeger *et al.*, 1995; Senesi *et al.*, 1976; Hori *et al.*, 1989).

For industrial purposes, prokaryotic PNPs are preferable as transglycosylation catalysts since they have a broader substrate specificity than the corresponding mammalian enzymes (Tonon *et al.*, 2004). Nevertheless, optimization of these enzymes for industrial use is desirable and involves *in vitro* approaches such as rational mutational active-site remodelling that depend on prior detailed knowledge of the molecular structures of progenitor enzymes. Furthermore, the molecular basis of the broader substrate specificity of hexameric PNPs compared with trimeric PNPs remains an unresolved question.

In this context, we have cloned, overexpressed, purified, crystallized and collected X-ray diffraction data for the hexameric purine nucleoside phosphorylase from *B. subtilis* strain 168, designated BsPNP233. Recently, it has been shown that BsPNP233 displays a relatively broad specificity and is able to catalyze the bioconversion of ribavirin, a nucleoside analogue with antiviral activity (Xie *et al.*, 2011). In addition, BsPNP233 has an optimal temperature of 323 K and is a good target for the catalysis of transglycosylation reactions using substrates whose solubility increases in hot aqueous solutions (Xie *et al.*, 2011; Visser *et al.*, 2010).

2. Materials and methods

2.1. Molecular cloning and expression

The short PNP comprising 233 amino-acid residues from *B. subtilis* strain 168 (BsPNP233; GenBank accession code AAB72065) was amplified from its genomic DNA by a standard PCR method using two oligonucleotide primers (forward, 5′-**CATATG**ATGAGTGTAC-ATATAGGTGCTG-3′; reverse 5′-**CTCGAG**TTATTGTGATACGG-AATGTAAA-3′). The amplified BsPNP233 gene was cloned into pGEM-T vector and further subcloned into the *Nde*I and *Xho*I restriction-enzyme sites of the pET-28a vector with a hexahistidine tag at the N-terminus. The resultant plasmid was transformed in *E. coli* Rosetta cells and plated on selective solid LB medium. One colony was picked up and grown in liquid LB–antibiotics for 16 h at 310 K and 200 rev min^{-1}. The culture was diluted to 2%(*v*/*v*) in fresh LB–antibiotics and grown under the same conditions to an $OD_{600\,nm}$ of 0.8. Expression of the recombinant protein was induced with 0.2 m*M* IPTG at 310 K for 4 h and the cells were harvested by centrifugation.

2.2. Purification

The harvested cells were resuspended in lysis buffer (50 m*M* Tris–HCl pH 7.4, 500 m*M* NaCl, 1 m*M* PMSF) and sonicated for 10 min with pulses of 4 s at 8 s intervals using a VC750 Ultrasonic Processor (Sonics Vibracell), setting the output amplitude to 60%. The cell debris solution was centrifuged at 10 000*g* for 30 min and the supernatant was loaded onto a nickel-affinity column (GE Healthcare) previously equilibrated with lysis buffer using an ÄKTA Fast Protein Liquid Chromatography (FPLC) system (GE Healthcare). The column was washed with five bed volumes of lysis buffer at a flow rate of 1.0 ml min^{-1}. The bound fractions were eluted using a non-linear gradient of 0.0–0.5 *M* imidazole in lysis buffer. The protein of interest was eluted with 200 m*M* imidazole and concentrated to 1 ml using Amicon centrifugal filter units (Millipore). The sample was submitted to size-exclusion chromatography (SEC) on a Superdex 200 column (GE Healthcare) pre-equilibrated with buffer consisting of 20 m*M* Tris–HCl pH 7.0, 50 m*M* NaCl, 1 m*M* DTT at a flow rate of 1.0 ml min^{-1}. Column calibration was performed in a buffer consisting of 20 m*M* Tris pH 7.4 with 200 m*M* NaCl at a flow rate of 1.0 ml min^{-1} using the following as standards: blue dextran 2000, ferritin (440 kDa), conalbumin (77 kDa), ovalbumin (45 kDa) and chymotrypsin (25 kDa). SDS–PAGE analysis (Laemmli, 1970) of the sample eluted from the Superdex 200 column confirmed its high degree of purity (Fig. 2). For crystallization trials, the sample was concentrated to 11 mg ml^{-1} using Amicon centrifugal filter units (Millipore). The protein concentration was determined by absorption spectroscopy at 280 nm using the theoretical molar extinction coefficient of 16 515 M^{-1} cm^{-1}, assuming that all cysteine residues form disulfide bonds.

2.3. Mass spectrometry

The protein band was excised, reduced, alkylated and submitted to in-gel digestion with trypsin. An aliquot (4.5 µl) of the resulting

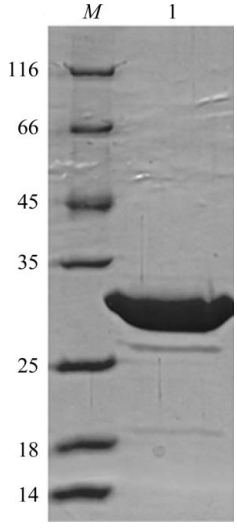

Figure 2
SDS–PAGE (13%) of purified BsPNP233 stained with Coomassie Brilliant Blue. Lane *M*, molecular-mass markers (kDa); lane 1, recombinant BsPNP233 purified by size-exclusion chromatography.

Table 1
Crystallization and preliminary X-ray diffraction analysis of different crystal forms of BsPNP233.

Values in parentheses are for the highest resolution shell.

Crystal	Form I	Form II	Form III	Form IV	Form V
Maximum dimension (µm)	250	150	400	550	500
Crystallization conditions	0.1 *M* sodium phosphate, 2 *M* ammonium sulfate, 5%(*v*/*v*) glycerol	0.1 *M* sodium acetate, 3.2 *M* sodium chloride, 5%(*v*/*v*) glycerol	0.1 *M* sodium citrate, 2 *M* ammonium sulfate, 0.2 *M* sodium–potassium tartrate	0.1 *M* HEPES, 1%(*v*/*v*) MPD, 2 *M* ammonium sulfate	0.1 *M* CAPS, 2 *M* ammonium sulfate, 0.2 *M* lithium sulfate, 5%(*v*/*v*) glycerol
pH	4.2	4.6	5.6	7.5	10.5
Space group	$P32_1$	$P6_322$	$P2_12_12_1$	$H32$	$H32$
Unit-cell parameters (Å, °)	$a = b = 136.83$, $c = 57.11$, $\alpha = \beta = 90$, $\gamma = 120$	$a = b = 135.81$, $c = 57.02$, $\alpha = \beta = 90$, $\gamma = 120$	$a = 56.74$, $b = 135.87$, $c = 236.40$, $\alpha = \beta = \gamma = 90$	$a = b = 158.26$, $c = 93.87$, $\alpha = \beta = 90$, $\gamma = 120$	$a = b = 158.53$, $c = 97.76$, $\alpha = \beta = 90$, $\gamma = 120$
Maximum resolution (Å)	2.35	2.65	1.71	1.70	2.10
R_{merge}†	9.2 (48.8)	10.0 (48.0)	6.5 (26.1)	9.3 (38.2)	10.7 (32.8)
$\langle I/\sigma(I)\rangle$	14.0 (3.8)	18.2 (3.8)	29.7 (5.8)	22.4 (4.6)	12.7 (3.7)
Completeness (%)	98.3 (97.4)	99.1 (99.9)	99.2 (95.4)	95.5 (92.6)	96.3 (97.1)
Multiplicity	7.6 (7.6)	6.4 (6.2)	7.6 (5.4)	8.0 (7.0)	5.7 (5.3)
Unique reflections	25344 (2478)	9359 (924)	196340 (18692)	47177 (4538)	26578 (2649)
Total reflections	192841	60155	1494607	375191	149883
V_M (Å^3 Da^{-1})	2.82	2.77	2.77/2.38/2.08	2.07	2.16
Molecules per AU‡	2	1	6/7/8	2	2

† $R_{merge} = \sum_{hkl}\sum_i |I_i(hkl) - \langle I(hkl)\rangle| / \sum_{hkl}\sum_i I_i(hkl)$, where $I_i(hkl)$ is the ith observation of reflection hkl and $\langle I(hkl)\rangle$ is the weighted average intensity for all i observations of reflection hkl. ‡ AU, asymmetric unit.

peptide mixture was separated by C18 (75 µm × 100 mm) RP-nanoUPLC (nanoAcquity, Waters) coupled with a Q-Tof Ultima mass spectrometer (Waters) with a nano-electrospray source at 0.6 µl min^{-1}. The gradient was 2–90%(*v*/*v*) acetonitrile in 0.1%(*v*/*v*) formic acid over 45 min. The instrument was operated in the 'top three' mode, in which one MS spectrum was acquired followed by MS/MS of the top three most intense peaks detected. The spectra were acquired using *MassLynx* v.4.1 software and the raw data files were converted to a peak-list format (mgf) by the *Mascot Distiller* v.2.3.2.0 software (Matrix Science Ltd) and searched against a non-redundant protein database (NCBI nr) using the *Mascot* v.2.3 engine (Matrix Science Ltd) with carbamidomethylation as a fixed modification, oxidation of methionine as a variable modification, one trypsin missed cleavage and a tolerance of 0.1 Da for both precursor and fragment ions.

2.4. Dynamic light scattering

Dynamic light-scattering (DLS) experiments were performed using a DynaPro 810 system (Protein Solutions) equipped with a Peltier temperature controller. An autopilot run with 50 measurements every 5 s was used. DLS experiments were carried out at 2.5 mg ml^{-1} protein concentration to verify aggregate formation and to estimate the hydrodynamic radius. DLS measurements were

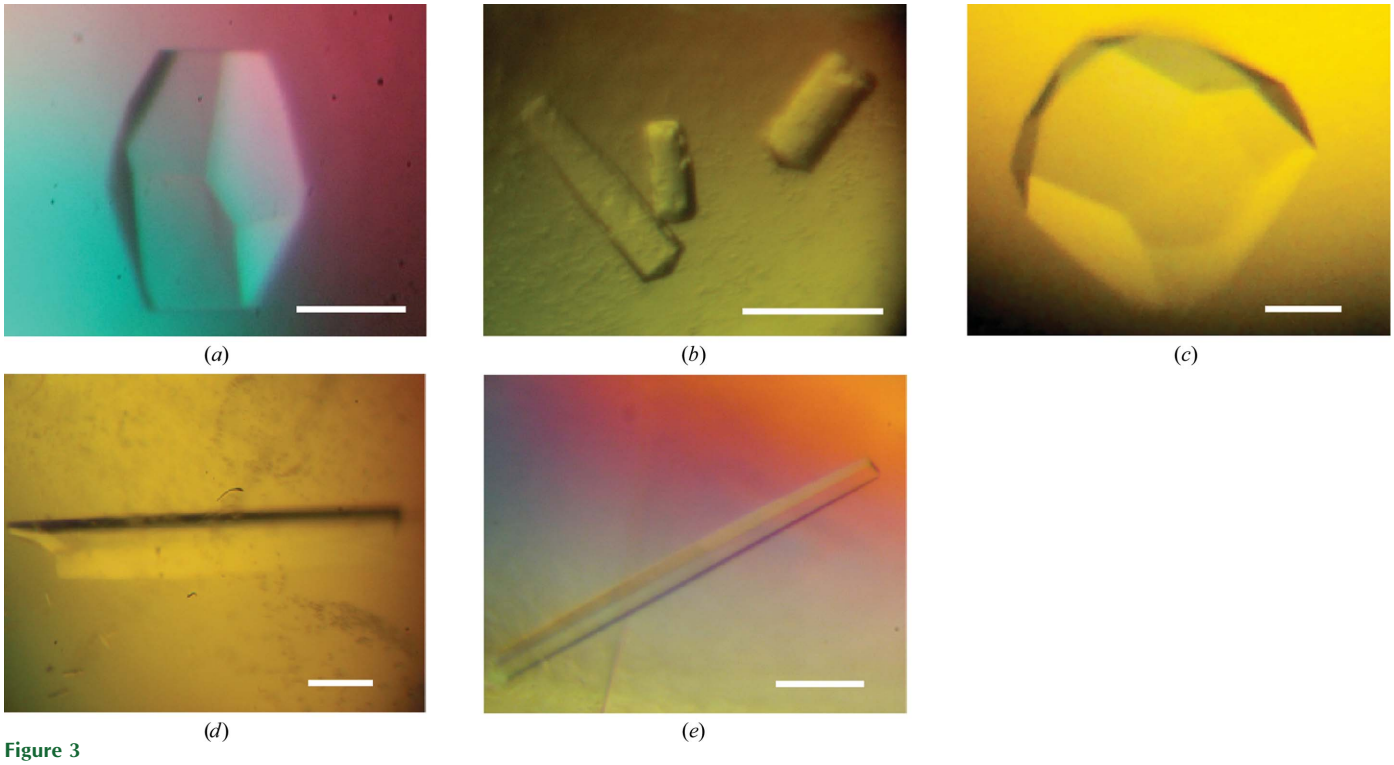

Figure 3
Crystals of BsPNP233. (*a*) Form I. (*b*) Form II. (*c*) Form III. (*d*) Form IV. (*e*) Form V. The scale bars are 100 µm in length.

conducted at 291 K. The samples to be analyzed were previously centrifuged. Hydrodynamic parameters were determined using the *DYNAMICS* v.6.3.40 software. The hydrodynamic radius (R_h) was extrapolated from the translational diffusion coefficient (D_t) using the Stokes–Einstein equation.

2.5. Crystallization

Crystallization experiments were performed by the sitting-drop vapour-diffusion method using a Cartesian HoneyBee 963 system (Genomic Solutions) at 291 K. A total of 544 different formulations based on commercial crystallization kits, including those from Hampton Research (SaltRx, Crystal Screen and Crystal Screen 2), Emerald BioSystems (Precipitant Synergy and Wizard I and II) and Qiagen/Nextal (PACT and JCSG+), were tested. For initial screening, a 0.5 µl volume of protein solution (at a concentration of 11 mg ml^{-1} in 20 m*M* Tris–HCl buffer pH 7.0, 50 m*M* NaCl, 1 m*M* DTT) was mixed with an equal volume of screening solution and equilibrated over a reservoir consisting of 80 µl of the latter solution. Crystals suitable for X-ray diffraction experiments were obtained from conditions from the initial screening (Fig. 3). Three of these were refined by adding 5%(*v*/*v*) glycerol to the mother liquor (Table 1). Crystals grew within 1–2 d to dimensions ranging from 0.1 to 0.5 mm depending on the crystal morphology.

2.6. X-ray diffraction analysis

X-ray diffraction experiments were conducted on the W01B-MX2 beamline at the Brazilian Synchrotron Light Laboratory (Campinas, Brazil). Diffraction data were collected from several crystals obtained from five different conditions after soaking in a cryoprotectant solution and further flash-cooling in a nitrogen-gas stream at 100 K. Interestingly, each condition resulted in crystals with different unit-cell parameters and the crystals had four different crystal symmetries. Data-collection strategies were designed depending on the crystal symmetry and maximum resolution. The radiation wavelength was set to 1.458 Å and a MAR Mosaic 225 mm CCD detector was used to record the X-ray diffraction data. The data were indexed, integrated and scaled using the *DENZO* and *SCALEPACK* programs from the *HKL*-2000 package (Otwinowski & Minor, 1997). Data-processing statistics are summarized in Table 1. Molecular-replacement calculations were performed using the *Phaser* (McCoy *et al.*, 2007) or *MOLREP* (Vagin & Teplyakov, 2010) programs.

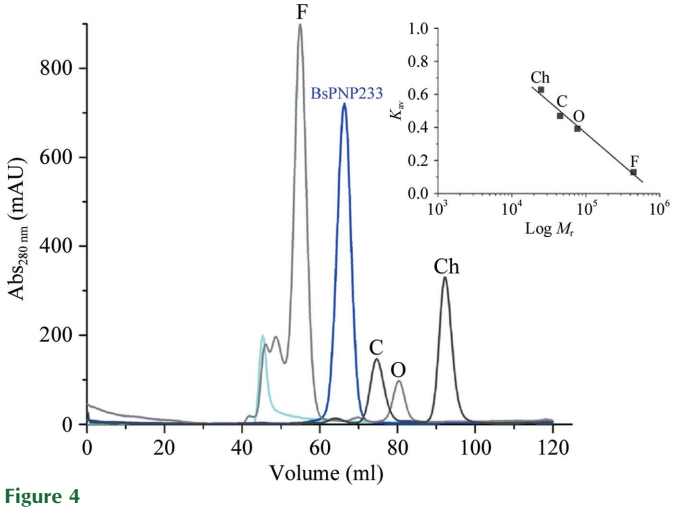

Figure 4
Analytical size-exclusion chromatography performed on a HiLoad 16/60 Superdex 200 pg column. The elution pattern of BsPNP233 is shown in blue, those of standard proteins in light or dark grey and that of blue dextran 2000 in cyan. Letters indicate the elution peaks of the standard proteins: F, ferritin (440 kDa); C, conalbumin (77 kDa); O, ovalbumin (45 kDa); Ch, chymotrypsin (25 kDa). The molecular mass estimated for BsPNP233 based on the calibration curve (inset) was 164 kDa, which is compatible with the theoretical mass for a hexamer (164.3 kDa). K_{av}, partition coefficient; M_r, relative molecular mass.

Table 2
Protein identification by LC-MS/MS for purine nucleoside phosphorylase from *B. subtilis* strain 168 (accession No. gi|16079021).

Peptide	*m*/*z*	*Z*
NAYDAAK	376.6763	2
VGSCGAIR	410.1728	2
NAYDAAKDK	498.2527	2
GMYGFTGTYK	562.7173	2
GQIADTVLLPGDPLR	782.9167	2
DVILAMTSSTDSQMNR	884.8794	2
VAFGSVDFAPCADFELLK	993.4664	2
VRDVILAMTSSTDSQMNR	675.3054	3
YGVLGVEMETTALYTLAAK	1015.5236	2
FIAETYLENVECYNEVR	1074.9704	2
ALSILTVSDHVLTGEETTAEER	791.0428	3
KALSILTVSDHVLTGEETTAEER	833.7664	3
GVPVTVGSVFTADQFYNDDSQIEK	1308.5884	2
DKGVPVTVGSVFTADQFYNDDSQIEK	953.7739	3

3. Results and discussion

The short PNP comprising 233 amino-acid residues from *B. subtilis* strain 168 was overexpressed and purified as a fusion with a synthetic amino-acid sequence (MGSSHHHHHHSSGLVPRGSH) corresponding to a 6×His tag and linker segment. Trypsin digestion of the purified protein and peptide analysis by mass spectrometry confirmed the identity of BsPNP233 (Table 2).

In order to investigate the oligomeric state of the recombinant BsPNP233, dynamic light-scattering (DLS), analytical size-exclusion chromatography (SEC) and small-angle X-ray scattering (SAXS) experiments were carried out. DLS experiments showed a monodispersive state (11% polydispersity) with a hydrodynamic radius (R_h) of 4.6 nm, which suggests the presence of hexamers in solution. The SEC analysis resulted in an apparent molecular mass of 164 kDa, which is compatible with the theoretical mass of hexameric BsPNP233 (164.2 kDa; Fig. 4). Moreover, preliminary SAXS data analysis by Guinier approximation resulted in a radius of gyration of 3.41 ± 0.01 nm, which is in good agreement with the R_g calculated for the crystallographic hexamer (3.40 nm).

Crystals were obtained using different chemical compounds as precipitant agents and at different pH values (Table 1; Fig. 3). They belonged to different crystal systems, including orthorhombic, trigonal and hexagonal. Examination of systematic absences in the reflections from the crystals obtained from conditions I, II and III indicated that they belonged to space groups $P32_1$, $P6_322$ and $P2_12_12_1$, respectively. The crystals from conditions IV and V belonged to either space group $H3$ or its enantiomorphic space group $H32$. The space-group ambiguity was solved in both cases after a translational search during molecular-replacement calculations, which showed that both belonged to space group $H32$.

Calculation of the Matthews coefficient (Matthews, 1968) based on the molecular mass of 27 377.9 Da indicated that crystal forms I, II, IV and V contained two, one, two and two molecules per asymmetric unit, respectively. For crystal form III, Matthews coefficient calculations indicated 6–8 molecules in the asymmetric unit. The statistics of data processing are summarized in Table 1.

Molecular replacement was carried out with the *Phaser* (McCoy *et al.*, 2007) or *MOLREP* (Vagin & Teplyakov, 2010) programs using the

(*a*) (*b*)

Figure 5
Crystal packing of BsPNP233 crystal forms. (*a*) illustrates the packing observed in crystal forms I, II and III, whereas (*b*) shows the crystal packing observed in crystal forms IV and V.

atomic coordinates of PNP from *B. anthracis* (PDB code 1xe3; Grenha *et al.*, 2005) as a search model.

The molecular-replacement calculations indicated that crystal form III contains six molecules per asymmetric unit and confirmed the numbers of molecules estimated from the Matthews coefficient (Matthews, 1968) for the other crystal forms. Rigid-body refinement of the best molecular-replacement solution for each crystalline system resulted in correlation coefficients of above 60% and crystallographic residuals of lower than 47%. Isotropic and restrained refinement with *REFMAC*5 (Murshudov *et al.*, 2011) and manual model building using *Coot* (Emsley & Cowtan, 2004) are currently in progress. Analysis of crystal packing only allowed identification of the hexamer in the asymmetric unit of crystal form III. In the other crystal forms the hexamer is reconstituted by applying the respective crystal symmetry operations. Considering the view presented in Fig. 5, the BsPNP233 crystal forms can be divided into two packing types (Fig. 5). Forms I, II and III present large solvent channels with hexagonal transverse sections, whereas forms IV and V display smaller solvent channels. These differences are attributed to distinct interfaces between neighbouring hexamers in the unit cell (Fig. 5).

PNPs are of great biotechnological importance owing to their potential application in the synthesis of nucleoside analogues used in the treatment of antiviral infections and in anticancer chemotherapy. The determination of crystal structures at different pH values ranging from 4.2 to 10.5 and in complex with substrate analogues might provide insights into their specificity and conformational stability, which will be instrumental in enzyme optimization and design, with the ultimate aim of economically viable biotechnological applications.

We gratefully acknowledge the Brazilian Biosciences National Laboratory (CNPEM, Campinas, Brazil) and Brazilian Synchrotron Light Laboratory (CNPEM, Campinas, Brazil) for the use of the crystallization (RoboLab), mass-spectrometry and X-ray diffraction (MX2 beamline) facilities. This research was supported by grants from Fundação de Amparo a Pesquisa do Estado de São Paulo (FAPESP) and Conselho Nacional de Desenvolvimento Científico e Tecnológico (CNPq).

References

Bzowska, A., Kulikowska, E. & Shugar, D. (2010). *Pharm. Ther.* **88**, 349–425.
De Clercq, E. (2009). *Int. J. Antimicrob. Agents*, **33**, 307–320.
Emsley, P. & Cowtan, K. (2004). *Acta Cryst.* D**60**, 2126–2132.
Grenha, R., Levdikov, V. M., Fogg, M. J., Blagova, E. V., Brannigan, J. A., Wilkinson, A. J. & Wilson, K. S. (2005). *Acta Cryst.* F**61**, 459–462.
Hori, H., Watanabe, M., Yamazaki, Y. & Mikami, Y. (1989). *Agric. Biol. Chem.* **53**, 3219–3224.
Koeller, K. M. & Wong, C.-H. (2001). *Nature (London)*, **409**, 232–240.
Laemmli, U. K. (1970). *Nature (London)*, **227**, 680–685.
Li, F., Maag, H. & Alfredson, T. (2008). *J. Pharm. Sci.* **97**, 1109–1134.
Matthews, B. W. (1968). *J. Mol. Biol.* **33**, 491–497.
McCoy, A. J., Grosse-Kunstleve, R. W., Adams, P. D., Winn, M. D., Storoni, L. C. & Read, R. J. (2007). *J. Appl. Cryst.* **40**, 658–674.
Murshudov, G. N., Skubák, P., Lebedev, A. A., Pannu, N. S., Steiner, R. A., Nicholls, R. A., Winn, M. D., Long, F. & Vagin, A. A. (2011). *Acta Cryst.* D**67**, 355–367.
Nannemann, D. P., Kaufmann, K. W., Meiler, J. & Bachmann, B. O. (2010). *Protein Eng. Des. Sel.* **23**, 607–616.
Otwinowski, Z. & Minor, W. (1997). *Methods Enzymol.* **276**, 307–326.
Pinheiro, E. dos S., Antunes, O. A. & Fortunak, J. M. (2008). *Antiviral Res.* **79**, 143–165.
Pugmire, M. J. & Ealick, S. E. (2002). *Biochem. J.* **361**, 1–25.
Ravandi, F. & Gandhi, V. (2006). *Expert Opin. Investig. Drugs*, **15**, 1601–1613.
Scheer, M., Grote, A., Chang, A., Schomburg, I., Munaretto, C., Rother, M., Söhngen, C., Stelzer, M., Thiele, J. & Schomburg, D. (2011). *Nucleic Acids Res.* **39**, D670–D676.
Seeger, C., Poulsen, C. & Dandanell, G. (1995). *J. Bacteriol.* **177**, 5506–5516.
Senesi, S., Falcone, G., Mura, U., Sgarrella, F. & Ipata, P. L. (1976). *FEBS Lett.* **64**, 353–357.
Tonon, G., Capra, E., Orsini, G. & Zuffi, G. (2004). US Patent 20040142438.
Vagin, A. & Teplyakov, A. (2010). *Acta Cryst.* D**66**, 22–25.
Visser, D. F., Hennessy, F., Rashamuse, K., Louw, M. E. & Brady, D. (2010). *Extremophiles*, **14**, 185–192.
Xie, X., Xia, J., He, K., Lu, L., Xu, Q. & Chen, N. (2011). *Biotechnol. Lett.*, doi:10.1007/s10529-011-0535-6.